

Prerake Diversity Combining for Pulsed UWB Systems Considering Realistic Channels with Pulse Overlapping and Narrow-Band Interference

Shiwei Zhao and Huaping Liu

School of Electrical Engineering and Computer Science

Oregon State University, Corvallis, OR 97331 USA

Email: hliu@eecs.orst.edu, Tel: +1 541 737 2973

Abstract—We analyze the prerake diversity combining schemes for pulsed ultrawideband (UWB) systems to shift the signal processing needs from the receiver to the transmitter. We consider the more realistic case that received multipath pulses could overlap with one another and its optimization based on the zero-forcing and the eigenanalysis technique. We show that in the presence of inter-pulse interference, the optimum linear prerake combining scheme in the sense of maximizing the received SNR performs the same as a conventional rake receiver with maximal ratio combining. Since for UWB systems it is important to consider the effects of narrow-band interference (NBI), we also analyze the different behaviors of prerake and rake schemes in the presence of NBI.

Index Terms – Ultrawideband, prerake combining, inter-pulse interference, narrowband interference.

I. INTRODUCTION

Ultrawideband (UWB) communications [1] could be achieved using the orthogonal frequency division multiplexing (OFDM) technique [2] or the pulsed technique [3]. One of the advantages of pulsed UWB is its ability to resolve individual multipath components. This requires a rake receiver [4], [5] to gain path diversity and to capture multipath energy.

Multipath combining using a rake structure requires multipath tracking and channel estimation. Hardware complexity, power consumption, and system cost scale up significantly with the number of paths combined, which should be avoided for portable or mobile units. Most UWB networks have fixed access points, and it is very desirable if the rake processes can be shifted from the mobile receivers to the transmitter at a fixed access point. As such a shift usually requires channel state information (CSI) in the transmitter, this technique is attractive for systems with time-division duplexing (TDD), where CSI can be easily obtained at both the transmitter and the receiver.

For TDD code-division multiple-access (CDMA) systems, a transmit precoding technique was investigated in [6]. This scheme suggests a prerake structure in which pre-delayed signal transmission is employed in the transmitter. This scheme was shown to have comparable performances with the common rake receivers. The prerake scheme has recently been applied to pulsed UWB systems [7], in which the ideal case that received adjacent paths are separated in time by at least one pulse width is assumed. This assumption might be acceptable for communications in line-of-sight (LOS) environments. In non-LOS indoor environments, however, it becomes inappropriate. For example, the typical average multipath arrival rate

is in the range of 0.5-2ns in the IEEE 802.15.3a channel model [10] and the pulse duration could be 2-4ns [12] for signals with a 10-dB bandwidth of 0.5-1GHz. Apparently, severe inter-pulse interference (IPI) could occur due to pulse overlapping. Besides IPI, co-existing narrow-band radios will interfere with UWB systems. The effects of narrowband interference (NBI) to UWB systems with rake reception have been analyzed extensively (e.g., [8], [9]). Prerake systems are expected to function differently from the conventional rake receiver in the presence of NBI. Therefore, the conclusions made in existing research on prerake UWB systems need to be re-examined and some optimizations might help to improve performance when IPI and NBI are taken into consideration.

In this paper, we study the structure, optimization, and performance of prerake UWB systems when IPI and NBI are taken into consideration. Background information such as the transmitted signal, UWB channel model, and the basic prerake scheme under ideal multipath resolution will be described in Section II. Section III discusses two optimization approaches at the transmitter to overcome IPI. Section IV addresses the effects of NBI. Simulation results for an indoor lognormal fading environment are provided in Section V to validate the analysis and to compare the performances of different algorithms in the absence or in the presence of IPI and NBI. Concluding remarks are given in Section VI.

II. PRERAKE DIVERSITY COMBINING

A. Transmitted signal and channel model

In pulsed UWB systems with binary pulse amplitude modulation (PAM), the amplitude of short-duration pulses is modulated by information bits. The transmitted signal without prerake processing is expressed as

$$s(t) = \sum_{i=-\infty}^{\infty} s_i(t) = \sum_{i=-\infty}^{\infty} \sqrt{E_b} b(i) p(t - iT_b) \quad (1)$$

where $p(t)$ is the UWB pulse shape of width T_p , E_b is the bit energy, T_b is the bit interval ($T_b \gg T_p$), and $b(i) \in \{1, -1\}$ is the i -th information bit. The energy of the basic pulse $p(t)$ is normalized to $E_p = \int_{-\infty}^{\infty} p^2(t) dt = 1$. $s(t)$ is then transmitted through an indoor multipath fading channel [10] with additive white Gaussian noise (AWGN). The channel for pulsed UWB systems can be modeled as a discrete linear filter with an

impulse response expressed as

$$h(t) = \sum_{l=0}^{L-1} \alpha_l \delta(t - \tau_l) \quad (2)$$

where L is the total number of multipath components, α_l is the channel fading coefficient for the l -th path, τ_l is the arrival time of the l -th path relative to the first path ($l = 0$ and $\tau_0 = 0$ assumed), and $\delta(t)$ is the Dirac delta function. When $|\tau_j - \tau_i| < T_p$, $i, j \in \{0, 1, \dots, L-1\}$, the i -th and the j -th received pulses overlap with each other and IPI occurs.

The channel gain α_l is modeled as $\alpha_l = \lambda_l \beta_l$, where $\lambda_l \in \{\pm 1\}$ with equal probability accounts for the random pulse inversion that could occur due to reflections [10]. The magnitude term β_l is modeled as having a lognormal distribution for indoor channels. The distribution of the path arrival time sequence τ_l and power delay profile of the channel are chosen to follow the modified Saleh-Valenzuela (S-V) model suggested in [10]. Because multipath components tend to arrive in clusters [10], τ_l in (2) is expressed as $\tau_l = \mu_c + \nu_{m,c}$, where μ_c is the delay of the c -th cluster that the l -th path falls in, $\nu_{m,c}$ is the delay (relative to μ_c) of the m -th multipath component in the c -th cluster. The relative power of the l -th path to the first path can be expressed as $E\{|\alpha_l|^2\} = E\{|\alpha_0|^2\} e^{-\mu_c/\Gamma} e^{-\nu_{m,c}/\gamma}$, where $E\{\cdot\}$ denotes expectation, Γ and γ are the cluster and path decay factors, respectively. Note that, different from the baseband models for narrow-band systems, α_l is real-valued in the UWB channel model [10]. We assume quasi-static fading, which allow channel coefficients α_l and relative delays τ_l to be constant over a block of data and change independently from one block to another.

B. Prerake model

The concept of prerake diversity combining was illustrated in [6], [7]. For completeness and for readers' convenience, we summarize the prerake model in this section. We assume that the signaling rate is such that the received signal energy of a particular bit is contained within one pulse repetition interval (T_b). Thus, there is no intersymbol interference (ISI) and we can focus on a particular bit interval in the receiver modeling. Corresponding to $s_i(t)$, which carries the i -th information bit given in (1), the received signal is expressed as

$$r(t) = \sum_{l=0}^{L-1} \alpha_l s_i(t - \tau_l) + n(t) \quad (3)$$

where $n(t)$ is the zero-mean white Gaussian noise process with a two-sided power spectral density (PSD) of $N_0/2$.

Assuming perfect channel knowledge, the correlator output of the l -th finger in a generic rake receiver that combines the first L_p ($L_p < L$) paths is expressed as

$$r_l = \sqrt{E_b} b(i) \sum_{k=0}^{L_p-1} \alpha_k \int_{-\infty}^{\infty} p(t - iT_b - \tau_k) p(t - iT_b - \tau_l) dt + n_l, \quad l = 0, 1, \dots, L_p - 1 \quad (4)$$

where the zero-mean noise component is $n_l = \int_{-\infty}^{\infty} n(t) p(t - iT_b - \tau_l) dt$ with variance $\sigma_{n_l}^2 = N_0/2$. For the ideal, non-realistic case when $|\tau_j - \tau_i| > T_p$, $i, j \in \{0, 1, \dots, L-1\}$,

received pulses do not overlap. Thus, all terms with $k \neq l$ in Eq. (4) equal zero, and r_l simplifies to

$$r_l = \alpha_l \sqrt{E_b} b(i) + n_l, \quad l = 0, 1, \dots, L_p - 1 \quad (5)$$

where noise components n_l are mutually independent.

In rake systems with linear combining, the decision variable is derived based on the outputs of the L_p rake fingers. Let $\mathbf{r} = [r_0, r_1, \dots, r_{L_p-1}]^T$ (where $(\cdot)^T$ denotes transpose), $\boldsymbol{\alpha} = [\alpha_0, \alpha_1, \dots, \alpha_{L_p-1}]^T$, and $\boldsymbol{\omega} = [\omega_0, \omega_1, \dots, \omega_{L_p-1}]^T$ be the tap weight vector for linear combining. The decision variable is expressed as $\Delta = \boldsymbol{\omega}^T \mathbf{r}$. It is well known that maximal ratio combining (MRC) is optimum when the desired signal is distorted only by AWGN. The MRC weights that maximize the output signal-to-noise ratio (SNR) are written as $\boldsymbol{\omega} = \boldsymbol{\alpha}^* = [\alpha_0, \alpha_1, \dots, \alpha_{L_p-1}]^H$, where $(\cdot)^*$ and $(\cdot)^H$ denote complex conjugate and Hermitian transpose, respectively. Note that although $\boldsymbol{\alpha}$ is a real vector given the models for UWB signals and channels described in Section II-A, Hermitian transpose, instead of transpose, is adopted because of its mathematical convenience.

In prerake systems, L_p pulses each scaled and delayed based on the multipath coefficients and delays are transmitted in each bit interval. The channel acts as a filter and convolves with the transmitted pulses. The scaling coefficients and relative delays are controlled such that the output peak of the correlator in the receiver is equivalent to the output of a conventional rake with MRC. This scheme is illustrated in Fig 1. Note that in

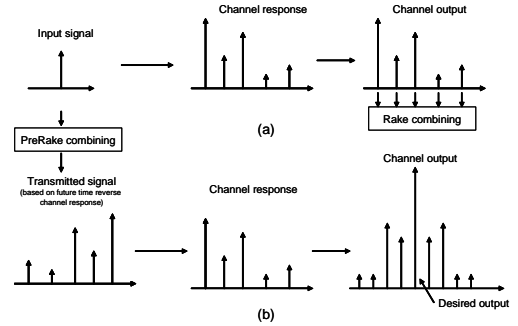


Fig. 1. Illustration of rake and prerake systems in the absence of pulse overlapping: (a) rake diversity combining; (b) prerake diversity combining.

the prerake system, the receiver requires only one correlator, correspondingly only symbol-rate processing, and does not need to perform channel estimation and multipath tracking.

Different from Eq. (1) for conventional rake systems, the transmitted signal (again, only the signal in the i -th bit interval is modeled) in a prerake system is expressed as

$$s'_i(t) = \sqrt{\frac{1}{\kappa}} \sum_{l=0}^{L_p-1} \alpha_{L_p-1-l}^* s_i(t - \tau_l) \quad (6)$$

where $\kappa = \boldsymbol{\alpha}^H \boldsymbol{\alpha}$ is a power normalization factor so that the transmitted bit energy remains E_b . After passing through the frequency-selective fading channel described by (2), $s'_i(t)$ arrives at the receiver as

$$r'(t) = \sqrt{\frac{E_b}{\kappa}} b(i) \sum_{l=0}^{L_p-1} \alpha_{L_p-1-l}^* \sum_{k=0}^{L_p} \alpha_k p(t - iT_b - \tau_l - \tau_k) + n(t). \quad (7)$$

As shown in Fig. 1, the receiver uses only the strongest path¹ to detect the i -th bit. The correlator output is expressed as

$$\Delta' = \int_{-\infty}^{\infty} r'(t)p(t - iT_b - \tau_{L_p-1})dt. \quad (8)$$

In the absence of pulse overlapping, Δ' simplifies to

$$\Delta' = \sqrt{\frac{E_b}{\kappa}} b(i) \sum_{l=0}^{L_p-1} \alpha_l^* \alpha_l + n' \quad (9)$$

where the zero-mean noise component $n' = \int_{-\infty}^{\infty} n(t)p(t - iT_b - \tau_{L_p-1})dt$ has a variance of $N_0/2$.

Let us examine the output SNR of the rake and prerake systems under the same transmitted bit energy. For the conventional rake system, let $\mathbf{n} = [n_0, n_1, \dots, n_{L_p-1}]^T$ be the noise vector. The instantaneous output SNR of the rake combiner is $\psi_{rake} = \frac{(\boldsymbol{\alpha}^H \boldsymbol{\alpha})^2 E_b}{2E\{\mathbf{n}^H \mathbf{n}\}}$, where $E\{\mathbf{n}^H \mathbf{n}\} = \boldsymbol{\alpha}^H \boldsymbol{\alpha} N_0/2$. In the receiver of the prerake system, the output signal energy is $\frac{(\boldsymbol{\alpha}^H \boldsymbol{\alpha})^2 E_b}{\kappa} = (\boldsymbol{\alpha}^H \boldsymbol{\alpha}) E_b$. Because there is no such a multipath combining process like in a rake system, not all the signal energy in the received multipath components are collected (only the strongest path is collected). However, the total noise energy scales down accordingly, $E\{n'^* n'\} = N_0/2$, so that the output SNR of prerake systems $\psi = \frac{E_b (\boldsymbol{\alpha}^H \boldsymbol{\alpha})}{N_0}$ equals to ψ_{rake} . Moreover, the rake and prerake systems have identical diversity orders, and thus the same error performance, which will be verified by simulation in Section V.

As indicated by Eq. (6), the energy for each bit is distributed in L_p pulses. Consequently, the maximum value of E_b in prerake systems could be as high as approximately L_p times of that in rake systems while still satisfying the FCC maximum instantaneous power requirements for UWB applications.

III. PRERAKE OPTIMIZATION IN THE PRESENCE OF IPI

Since pulse overlapping causes IPI, Eqs. (5) and (9) do not hold anymore. Following the notation used in [13], we define the partial correlation between $p(t - \tau_k)$ and $p(t - \tau_l)$ as $\rho_{l,k} = \int_{-\infty}^{\infty} p(t - \tau_l)p(t - \tau_k)dt = \rho_{k,l}$. Since the energy of $p(t)$ is normalized to unity, $\rho_{l,k} = 1$ for $l = k$ and $0 \leq |\rho_{l,k}| < 1$ for $l \neq k$. Note that $\rho_{l,k} = 0$ if $p(t - \tau_k)$ and $p(t - \tau_l)$ are mutually orthogonal or do not overlap with each other.

For rake receivers derived from the signal model given in (4), the received signal vector becomes

$$\mathbf{r} = \sqrt{E_b} b(i) \mathbf{R} \boldsymbol{\alpha} + \mathbf{n} \quad (10)$$

where

$$\mathbf{R} = \begin{bmatrix} 1 & \rho_{0,1} & \dots & \rho_{0,L_p-1} \\ \rho_{1,0} & 1 & \dots & \rho_{1,L_p-1} \\ \vdots & \vdots & \ddots & \vdots \\ \rho_{L_p-1,0} & \rho_{L_p-1,1} & \dots & 1 \end{bmatrix} \quad (11)$$

is the partial correlation matrix, which can be calculated using the relative multipath delays τ_l and the pulse shape $p(t)$. Thus, the zero-mean noise components at the output of different receiver fingers are not independent anymore, and the covariance matrix of \mathbf{n} (zero mean) is obtained to be

¹The L_p -th path whose delay relative to the first-arriving path is τ_{L_p-1} .

$E\{\mathbf{n} \mathbf{n}^H\} = \mathbf{R} \frac{N_0}{2}$. The decision variable is still $\Delta = \mathbf{w}^T \mathbf{r}$. Note that in the model given by Eqs. (10) and (11), the effect due to the potential overlap from statistically weaker paths L_p, \dots, L has been neglected.

In the presence of pulse overlapping, it should be mentioned that the ideal case shown in Fig. 1 must be modified accordingly. Due to IPI and the non-uniform time intervals between different multipath components, the appearance of the channel outputs at the receiver frontend as shown in Fig. 2 is very different from that shown in Fig. 1. However, the desired output signal components at the correlation peak are the same for both cases.

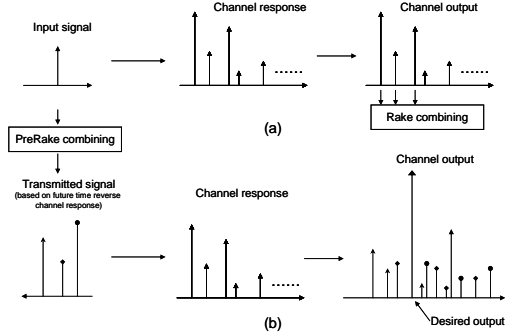


Fig. 2. Concept of prerake systems in the presence of pulse overlapping: (a) rake diversity combining; (b) prerake diversity combining.

Because of the noise correlation and the additional distortion to received signals caused by IPI, prerake combining schemes designed according to the MRC rule may not be optimum. For prerake systems, we define the scaling factor for pulses constituting $s'_i(t)$ as $\mathbf{w} = [w_0, w_1, \dots, w_{L_p-1}]^T$. Thus $s'_i(t)$ is re-written as

$$s'_i(t) = \sqrt{\frac{1}{\kappa}} \sum_{l=0}^{L_p-1} \mathbf{w}_{L_p-1-l} s_i(t - \tau_l) \quad (12)$$

where the power normalization factor becomes $\kappa = \mathbf{w}^H \mathbf{R} \mathbf{w}$. Correspondingly, Eq. (9) becomes

$$\Delta' = \sqrt{\frac{E_b}{\kappa}} b(i) \mathbf{w}^T \mathbf{R} \boldsymbol{\alpha} + n'. \quad (13)$$

The choices of the prerake tap weight vector \mathbf{w} should be investigated for better performance.

A. Zero-forcing optimization

From (13), a natural choice of the prerake weight vector \mathbf{w} to overcome the effect of IPI is to apply the zero forcing (ZF) scheme, which yields a weight vector

$$\mathbf{w}^T = \boldsymbol{\alpha}^H \mathbf{R}^{-1} \quad (14)$$

where the matrix inversion always exists since \mathbf{R} is a positive definite Hermitian matrix. With the ZF prerake combining weight, $\mathbf{w}^T \mathbf{R} \boldsymbol{\alpha} = \boldsymbol{\alpha}^H \boldsymbol{\alpha}$, and IPI is completely removed in the received signal.

It is well known that applying a ZF filter to remove interference in a rake receiver will enhance the additive noise. For prerake combining, since the ZF filtering is done at the

transmitter, there is no noise enhancement. However, applying the ZF combining weight \mathbf{w} in prerake systems increases the power normalization factor κ , except when \mathbf{R} is an identity matrix (no pulse overlapping). This will effectively lower the received SNR since the average transmitted signal power must be kept constant.

B. Maximization of the received SNR based on eigenanalysis

The optimum diversity combining in the sense of maximizing the received SNR in a prerake system is to find \mathbf{w} that maximizes ψ . With the quasi-static model adopted for slowly fading channels, the channel fading coefficients and relative path delays are static over a block of data. Next, we apply the eigenanalysis method to maximize the instantaneous SNR in each block to achieve optimum system performance.

As easily seen from Eq. (13), now the correlator output SNR of a prerake system in the presence of IPI becomes $\psi = \frac{E_b \mathbf{w}^T \mathbf{R} \boldsymbol{\alpha} \boldsymbol{\alpha}^H \mathbf{R}^H \mathbf{w}^*}{\kappa N_0}$. Maximizing ψ is equivalent to maximizing $\psi' = \frac{\mathbf{w}^T \mathbf{R} \boldsymbol{\alpha} \boldsymbol{\alpha}^H \mathbf{R}^H \mathbf{w}^*}{\kappa} = \frac{\mathbf{w}^T \mathbf{R} \boldsymbol{\alpha} \boldsymbol{\alpha}^H \mathbf{R}^H \mathbf{w}^*}{\mathbf{w}^T \mathbf{R} \mathbf{w}^*}$. From Eq. (11), we know that matrix \mathbf{R} is Hermitian and positive definite. By using Cholesky factorization, \mathbf{R} can be expressed as $\mathbf{R} = \mathbf{M}^H \mathbf{M}$. If we define a new vector $\mathbf{u} = \mathbf{M} \mathbf{w}^*$, ψ' can be re-written as $\frac{\mathbf{u}^H \mathbf{M} \boldsymbol{\alpha} \boldsymbol{\alpha}^H \mathbf{M}^H \mathbf{u}}{\mathbf{u}^H \mathbf{u}}$. From the minimax theorem in eigenanalysis [14], the optimum prerake combining vector

$$\mathbf{u} = \underset{\mathbf{u}}{\operatorname{argmax}} \left\{ \frac{\mathbf{u}^H \mathbf{M} \boldsymbol{\alpha} \boldsymbol{\alpha}^H \mathbf{M}^H \mathbf{u}}{\mathbf{u}^H \mathbf{u}} \right\} \quad (15)$$

is the principal eigen vector (the eigen vector corresponding to the largest eigen value) of $\mathbf{M} \boldsymbol{\alpha} \boldsymbol{\alpha}^H \mathbf{M}^H$. Because $\mathbf{M} \boldsymbol{\alpha} \boldsymbol{\alpha}^H \mathbf{M}^H = \mathbf{M} \boldsymbol{\alpha} (\mathbf{M} \boldsymbol{\alpha})^H$ is formed from a single column vector $\mathbf{M} \boldsymbol{\alpha}$, it is of only rank 1 with only one non-zero eigen value corresponding to the principal eigen vector $\mathbf{v} = \mathbf{M} \boldsymbol{\alpha}$. We let $\mathbf{u} = \mathbf{v}$, which apparently leads to the conclusion that $\mathbf{w} = \boldsymbol{\alpha}^*$.

This implies that, interesting although unexpected, even in the presence of IPI, MRC is still the optimum linear prerake diversity combining scheme. This choice of the prerake combining weight ($\mathbf{u} = \mathbf{M} \boldsymbol{\alpha}$ and \mathbf{M} is obtained by applying Cholesky decomposition of \mathbf{R}) results in the same error performance as a conventional rake receiver with MRC when IPI is present.

IV. THE EFFECTS OF NARROW-BAND INTERFERENCE

Prerake and rake systems may perform differently in the presence of narrowband interference. This is because the receiver of a prerake system takes only one sample per bit for detection whereas the receiver of a rake system needs L_p samples. For simplicity, we consider the case that there is only one NBI source. The observations drawn from this case are applicable to the scenario of multiple independent NBI sources. Let $I(t)$ represent the interference signal. The correlator output for the i -th information bit of a prerake system when NBI is present is modified as

$$\Delta' = \sqrt{\frac{E_b}{\kappa}} b(i) \mathbf{w}^T \mathbf{R} \boldsymbol{\alpha} + n' + I' \quad (16)$$

where $I' = \int_{-\infty}^{\infty} I(t) p(t - iT_b - \tau_{L_p-1}) dt$.

The narrowband interference does not change the weight selection for prerake diversity combining. For the ZF optimization, noises are not taken into consideration. For the eigenanalysis-based SNR maximization, the instantaneous SNR must be modified as $\psi = \frac{E_b \mathbf{w}^T \mathbf{R} \boldsymbol{\alpha} \boldsymbol{\alpha}^H \mathbf{R}^H \mathbf{w}^*}{\kappa(N_0 + E_I)}$, where E_I is the instantaneous NBI energy collected by the receiver. Since E_I is independent of the weight vector \mathbf{w} , NBI does not change the weight optimization process for prerake multipath diversity combining.

As concluded in Section III, rake and prerake systems with MRC have the same error performance when only AWGN is present. However, the NBI terms in the decision variables of rake and prerake receivers have different distributions, which may result in different error performances for the two schemes. Let us examine the NBI terms in the decision variables for rake and prerake schemes. When NBI is present, the combiner output of a common rake receiver given in (16) must be modified as

$$\Delta = \sqrt{E_b} b(i) \mathbf{w}^T \mathbf{R} \boldsymbol{\alpha} + \sum_{l=0}^{L_p-1} w_l n_l + \sum_{l=0}^{L_p-1} w_l I_l \quad (17)$$

where $I_l = \int_{-\infty}^{\infty} I(t) p(t - iT_b - \tau_l) dt$. To make the comparison fair, fading, AWGN, and NBI experienced by both the rake and prerake systems must be kept the same. For all practical scenarios, the time-span of the L_p paths is much shorter than the coherence time of the narrowband interference waveforms. It is thus reasonable to assume that $I_l \approx I'$, $l = 0, \dots, L_p-1$. For prerake systems, NBI experienced by the receiver only depends on NBI $I(t)$ and UWB pulse shape $p(t)$, as clearly seen from I' defined in (16). For rake systems, the elements of the multipath combining \mathbf{w} (equals $\boldsymbol{\alpha}^*$ if MRC is adopted) are random variables. Therefore, as clearly seen from (17), besides $I(t)$ and $p(t)$, the distribution of NBI experienced by the receiver also depends on the distribution of $\sum_{l=0}^{L_p-1} w_l$.

These differences are illustrated via simulation for which NBI is generated by filtering a sequence of non-return-to-zero converted random binary bits with a square-root raised cosine (RRC) filter with a 3-dB bandwidth of 1MHz and energy of $25E_b$. In all cases, $E \left\{ \sum_{l=0}^{L_p-1} |\alpha_l|^2 \right\} = 1$ is maintained for the UWB channel. The distribution of NBI experienced by a rake and a prerake system when NBI is not faded is shown in Fig. 3. In a more realistic scenario, NBI arrives at a rake or prerake receiver through a fading channel. Because at a same time NBI experienced by prerake or rake system always has same level of fading, Fig. 3 is sufficient to illustrate the fundamental difference of their distributions.

V. SIMULATION RESULTS AND DISCUSSION

In obtaining simulation results, a carrier-modulated, truncated Gaussian pulse is applied as the UWB pulse shape $p(t)$. This pulse has a width of $T_m = 1ns$ and a 10-dB bandwidth of 2GHz. We adopt the CM3 channel model [10] with a root-mean-square (RMS) delay spread of $15ns$, an average cluster arrival rate of $0.0667/ns$, and an average path arrival rate of $2/ns$. The cluster and path decay factors applied are $\Gamma = 14ns$ and $\gamma = 7.9ns$, respectively. The standard deviation of fading coefficients is 3.4dB. The total collected energy by L_p fingers

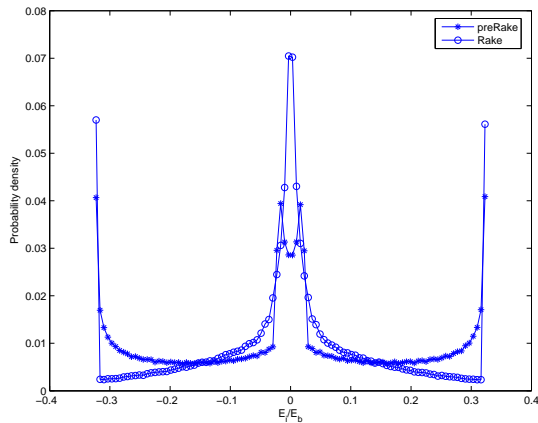


Fig. 3. Distributions of NBI experienced by prerake and rake systems when NBI is not faded.

is normalized as $E\{\sum_{l=0}^{L_p-1} |\alpha_l|^2\} = 1$, where $L_p = 5$. The transmission rate $1/T_b$ is such that inter-symbol interference caused by channel excess delay is negligible. Also, the receiver is assumed to have perfect knowledge of the channel.

Fig. 4 shows the simulated error performances of prerake and rake systems in the absence or presence of IPI. All parameters of the channel and transmitted signals are the same for the IPI and non-IPI cases, except that the path arrival rate for the non-IPI case is controlled so that no IPI occurs. It is observed that although IPI degrades the performance, both the prerake and rake systems with MRC combining perform the same. When there is no pulse overlapping, the ZF scheme for prerake system is same as MRC. In the presence of pulse overlapping, however, the ZF optimization for prerake multipath combining performs worse than the MRC scheme for reasons as explained in Section III.

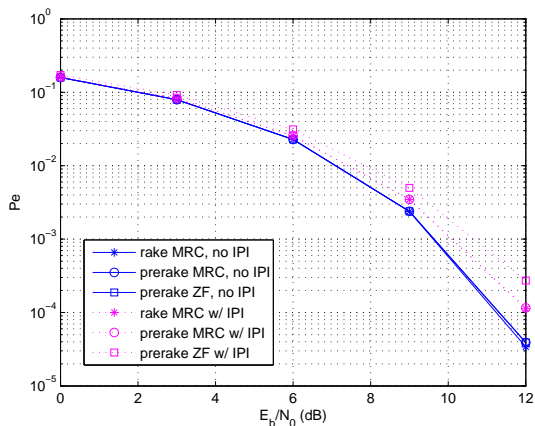


Fig. 4. Simulated BER versus E_b/N_0 curves of the prerake and rake systems with and without IPI, in the absence of NBI.

Error performance in the presence of NBI is shown in Fig. 5. NBI signals are generated using the method described in Section IV. It is observed that in the presence of NBI the prerake scheme performs better than the traditional rake scheme. This is caused by the different distributions of NBI experienced by the two systems as shown in Fig. 3.

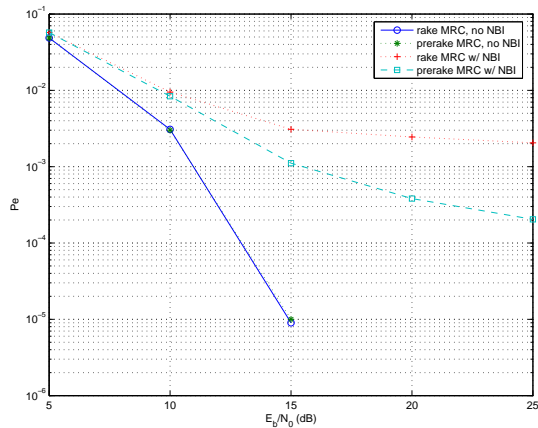


Fig. 5. Simulated BER versus E_b/N_0 curves of the prerake and rake systems with and without NBI, in the absence of IPI.

VI. CONCLUSION

Optimization of prerake multipath combining schemes has been discussed for pulsed UWB in the presence of IPI. MRC is still proved to be the optimum linear multipath combining scheme in the sense of maximum received SNR. We have also assessed the receiver behavior and performance of both the prerake and the traditional rake schemes in the presence of NBI. The prerake scheme has been found to outperform the rake scheme when NBI is present.

REFERENCES

- [1] FCC notice of proposed rule making, "Revision of part 15 of the commission's rules regarding ultra-wideband transmission systems," ET-Docket 98-153.
- [2] J. Balakrishnan, A. Batra, and A. Dabak, "A multi-band OFDM system for UWB communication," in *Proc. IEEE UWBST*, Nov. 2003.
- [3] M. Z. Win and R. A. Scholtz, "Impulse radio: how it works," *IEEE Commun. Lett.*, vol. 2, pp. 36–38, Feb. 1998.
- [4] M. Z. Win and R. A. Scholtz, "On the energy capture of ultrawide bandwidth signals in dense multipath environments," *IEEE Commun. Lett.*, vol. 2, pp. 245–247, Sep. 1998.
- [5] S. Gaur and A. Annamalai, "Improving the range of UWB transmission using RAKE receivers," in *Proc. IEEE VTC 2003-Fall*, Oct. 2003, pp. 597–601.
- [6] R. Esmailzadeh, E. Sourour, and M. Nakagawa, "Prerake diversity combining in time-division duplex CDMA mobile communications," *IEEE Trans. Veh. Technol.*, vol. 48, pp. 795–801, May 1999.
- [7] K. Usuda, H. Zhang, and M. Nakagawa, "Pre-Rake performance for pulse based UWB system in a standardized UWB short-range channel," in *Proc. IEEE WCNC'04*, vol. 2, Mar. 2004.
- [8] L. Zhao and A. M. Haimovich, "Performance of ultra-wideband communications in the presence of interference," *IEEE J. Sel. Areas Commun.*, vol. 20, pp. 1684–1691, Dec. 2002.
- [9] J. R. Foerster, "The performance of a direct-sequence spread ultra-wideband system in the presence of multipath, narrowband interference and multiuser interference," in *Proc. IEEE UWBST*, May 2002, pp. 87–91.
- [10] A. F. Molisch, J. R. Foerster, and M. Pendergrass, "Channel models for ultrawideband personal area networks," *IEEE Wireless Commun.*, vol. 10, pp. 14–21, Dec. 2003.
- [11] S. Zhao, H. Liu, and S. Mo, "Performance of a multi-band ultra-wideband system over indoor wireless channels," in *Proc. IEEE CCNC'04*, Jan. 2004.
- [12] M. Hamalainen, V. Hovinen, R. Tesi, J. H. J. Inatti, and M. Latva-aho, "On the UWB system coexistence with GSM900, UMTS/WCDMA, and GPS," *IEEE J. Sel. Areas Commun.*, vol. 20, pp. 1712–1721, Dec. 2002.
- [13] S. Zhao and H. Liu, "On the optimum linear receiver for impulse radio system in the presence of pulse overlapping," *IEEE Commun. Lett.*, vol. 9, pp. 340–342, Mar. 2005.
- [14] S. Haykin, *Adaptive filter theory*. Prentice Hall, New Jersey, 1996.